APPENDIX G:

CSEM BASELINE SUMMARY REPORT

Turkey Point Cooling Canal System
Baseline CSEM Report

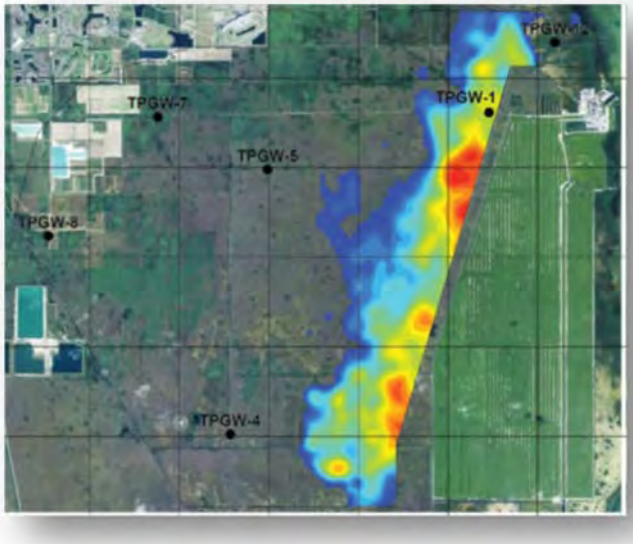

1.0 Executive Summary

Pursuant to the FDEP Consent Order requirements of paragraph 29(a), and as outlined in item (3b) in the MDC letter dated May 15, 2017, FPL conducted a baseline Continuous Surface Electromagnetic Mapping (CSEM) survey to map the hypersaline plume adjacent to the Turkey Point Plant. The following provides CSEM survey information that will be used as the baseline characterization of the hypersaline plume volume and location at the initiation of the Recovery Well System operation on May 15, 2018. The CSEM survey was conducted in Month 2018 by Enercon Services, Inc., the same firm that conducted the original CSEM survey of 2016.

2.0 Background

The baseline CSEM survey area encompassed approximately 30 square miles of mostly submerged and partially submerged land surface, generally to the west and north of the CCS. Figure 2.0 presents the Turkey Point facility, CCS and coverage area for the CSEM survey. The 2018 baseline CSEM survey was performed using the same airborne platform and electromagnetic technique used for the 2016 survey, a helicopter-borne Time Domain Electromagnetic (TEM) system developed and implemented by SkyTEM Canada, Inc. (SkyTEM), and provided nearly continuous EM survey data within the coverage area.

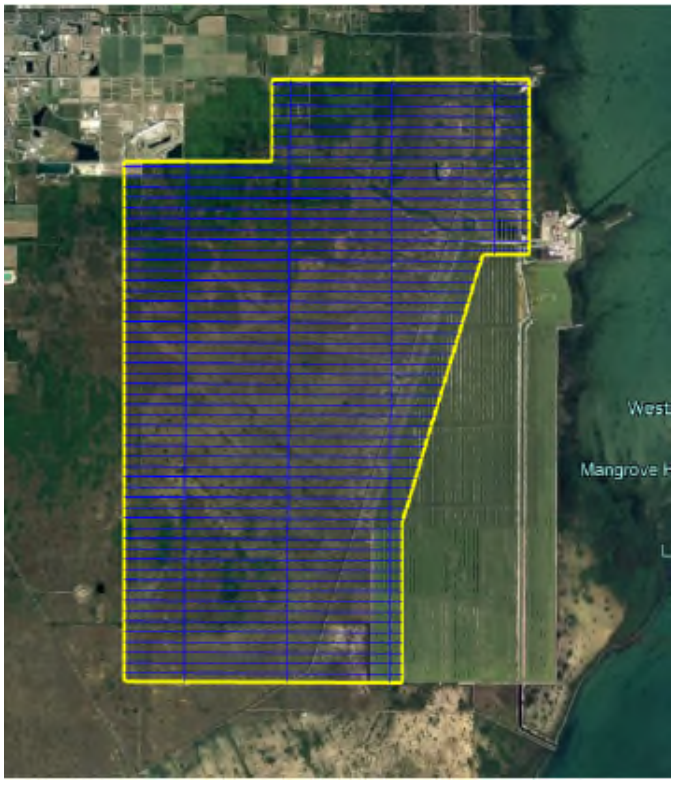

Figure 2.0 CSEM Survey Area (within yellow border) at the Turkey Point Site. Individual transects are shown west to east in blue.

2.1 Approach and Methods

The information is collected using TEM sounding equipment suspended from an airborne platform that conducts prescribed flight lines (transects) over the target area. In this application the individual transects run from west to east (as shown in Figure 2-0) and cover the entire region of interest.

The CSEM survey measures bulk conductivity of groundwater to assess the vertical and horizontal extent of a hypersaline plume in the groundwater in the vicinity of the CCS. When pore water chloride ion content is high, bulk conductivity and fluid conductivity have a nearly 1:1 relationship. This allows the measurement of fluid conductivity from bulk resistivity or conductivity values obtained from geophysical surveys. The high electrical conductivity of saline groundwater makes it an excellent target for electrical geophysical methods. However, as a result of lithologic effects, the relationship between bulk electrical properties and fluid conductivity must be calibrated with local water quality data. ENERCON established a relationship for the Biscayne Aquifer near the CCS during performance of the initial 2016 CSEM survey as reported in "PTN Cooling Canal System, Electromagnetic Conductance Geophysical Survey, DRAFT FINAL REPORT, Florida Power and Light Turkey Point Power Plant, 9700 SW 433th Street, Homestead, FL 33035" (ENERCON, 2016). The process conducted by ENERCON in 2016 and for this report, follows the USGS method previously conducted for the Biscayne (Prinos, et al., 2014).

2.2 Conversion of CSEM Resistivity to Estimated Chlorinity of Ground Water

Quarterly water quality data from the TPGW monitor wells were used to develop an equation for conversion of CSEM resistivity to equivalent groundwater chloride ion content (chlorinity). Water quality sample results dated September 2015 and March 2018 collected from the TPGW monitor wells were used for this analysis (Tables 1 and 2). Normal seawater has a salinity of about 35 practical salinity units (psu) and will have a chlorinity of about 19,000 mg/L. DERM delineates 19,000 mg/L chloride to be the boundary between normal salinity seawater or brackish waters and hypersaline groundwater. Chloride concentrations greater than 19,000 mg/L traditionally equate to salinity greater than 35 psu.

Table 1. September 2015 Water Quality data from TPGW wells used for Calibration

	Well Screen (from Top of Casing)								
WELL_ID	From (ft)	To (ft)	From (m)	To (m)	Cl (mg/L)	Na (mg/L)	TDS (mg/L)	Salinity (PSU)	Specific Conductance (µS/cm)
TPGW-1	26.99	29.00	8.23	8.84	21200	11800	37200	38.909	58381
TPGW-1	47.99	49.99	14.63	15.24	26700	14500	39600	48.97	71423
TPGW-1	79.97	83.97	24.38	25.6	27000	14800	48200	50.08	72806
TPGW-4	22.50	24.50	6.86	7.47	487	244	1150	1.12	2195
TPGW-4	37.98	42.97	11.58	13.1	12900	7530	24500	25.8	40457
TPGW-4	61.96	65.99	18.89	20.12	15500	8250	26600	27.52	42850
TPGW-5	24.01	27.98	7.32	8.53	151	74.4	526	0.49	999
TPGW-5	45.00	49.99	13.72	15.24	10700	5870	18000	19.7	31646
TPGW-5	62.48	67.47	19.05	20.57	11800	6700	21100	22.71	35991
TPGW-7	22.01	25.98	6.71	7.92	36.7	21.1	298	0.28	572
TPGW-7	47.99	51.96	14.63	15.84	37.799	21.2	314	0.28	584
TPGW-7	79.97	83.97	24.38	25.6	2130	876	5100	3.75	6840
TPGW-8	16.99	20.99	5.18	6.4	31.8	17.1	216	0.21	444
TPGW-8	35.00	37.00	10.67	11.28	31.8	17.6	360	0.31	643
TPGW-8	49.50	53.50	15.09	16.31	43	25.2	382	0.34	705
TPGW-12	22.01	23.98	6.71	7.31	16300	9480	29200	30.93	47659
TPGW-12	55.99	59.99	17.07	18.29	23000	12800	41200	41.99	62472
TPGW-12	89.97	93.97	27.43	28.65	23700	14100	41500	44.4	65603

Table 2. March 2018 Water Quality data from TPGW wells used for Calibration

WELL_ID	WellScreen (from Top of Casing)				Cl (mg/L)	Na (mg/L)	TDS (mg/L)	Salinity (PSU)	Specific Conductance (µS/cm)
	From (ft)	To (ft)	From (m)	To (m)					
TPGW-1	32.00	34.00	9.76	10.37	19400	10000	34000	32.37	49560
TPGW-1	52.10	54.10	15.88	16.49	27700	14400	51200	48.46	70730
TPGW-1	85.30	89.30	26.01	27.23	28500	14500	51800	48.03	70175
TPGW-2	27.97	31.97	8.53	9.75	24800	13100	44400	50.89	73809
TPGW-2	53.88	55.88	16.43	17.04	29500	15700	52800	51.56	74653
TPGW-2	88.79	90.79	27.07	27.68	31300	15300	52400	42.78	63424
TPGW-4	23.20	25.20	7.07	7.68	2280	1100	4320	4.08	7407
TPGW-4	38.10	43.10	11.62	13.14	15100	7550	27400	25.38	39803
TPGW-4	61.60	65.60	18.78	20.00	14800	7880	27500	26.34	41164
TPGW-5	28.60	32.60	8.72	9.94	164	84.6	550	0.47	958
TPGW-5	49.30	54.30	15.03	16.55	11700	6070	22800	21.39	34108
TPGW-5	67.00	72.00	20.43	21.95	13100	7110	22900	23.08	36531
TPGW-6	25.09	27.09	7.65	8.26	313	150	940	0.76	1518
TPGW-6	51.61	55.61	15.73	16.95	7970	4040	14300	13.78	22822
TPGW-6	84.70	88.70	25.82	27.04	8670	4230	14700	14.66	24164
TPGW-12	25.19	27.19	7.68	8.29	16500	9000	31600	30.75	47355
TPGW-12	59.21	63.21	18.05	19.27	20900	11500	39500	39.44	59098
TPGW-12	93.24	97.24	28.43	29.65	24000	12900	48200	44.13	65218
TPGW-15	24.32	29.32	7.41	8.94	20100	10500	ND	33.07	50575
TPGW-15	44.39	49.39	13.53	15.06	30000	15600	ND	49.02	71547
TPGW-15	79.31	84.31	24.18	25.70	28800	17400	ND	50.77	73747
TPGW-17	32.11	37.11	9.79	11.31	24900	12300	43000	42.57	63088
TPGW-17	49.95	54.95	15.23	16.75	29300	15200	55400	49.89	72514
TPGW-17	86.81	91.81	26.47	27.99	28600	14400	48000	48.01	70094
TPGW-18	35.25	40.25	10.75	12.27	14200	7220	25000	22.57	35844
TPGW-18	63.25	68.25	19.28	20.81	25200	13600	44200	40.71	60684
TPGW-18	84.27	91.27	25.69	27.83	26400	14800	42600	42.12	62531
TPGW-19	27.37	31.37	8.34	9.56	1830	1070	3600	3.37	6194
TPGW-19	48.39	52.39	14.75	15.97	26000	13500	42200	39.18	58599
TPGW-19	84.35	89.35	25.72	27.24	26800	13700	41200	40.76	60679

The calibration of the CSEM data was conducted using a two-step approach as presented in Fitterman and Prinos (2011) and Fitterman et al. (2012). First, a mathematical relationship was established between CSEM resistivity and the resistivity of groundwater samples from discrete depth intervals in the TPGW monitor wells (water resistivity is the inverse of specific conductance). The mean values of the CSEM resistivities within the 150-meter radius (492 feet) of each corresponding TPGW monitor well were selected to integrate the footprint of the CSEM system and to develop a statistical range in bulk resistivities for the model layer that was at an equivalent depth to the screened intervals in the TPGW wells.

The data are plotted on a log-log plot with the mean CSEM resistivity on the x-axis and groundwater laboratory sample resistivity on the y-axis. A regression equation is fitted to the plot to produce a power function of the form:

$$Water\ Resistivity = 0.0843 \cdot (CSEM\ Resistivity)^{1.1784} \qquad (1)$$

with $R^2 = 0.91$, $p < 0.001$, $r = 0.95$. The p value measures the probability that the observed relationship is due to random variation, R^2 is the percent of the variance in the dependent variable (water resistivity) explained by the variance of the independent variable (CSEM resistivity), and r is a measure of the correlation between groundwater resistivity and CSEM resistivity with 0.95 indicating a very strong, nearly perfect, correlation. This is an expected relationship as the groundwater samples are from one hydrogeologic unit, the Biscayne Aquifer, and bulk resistivity (CSEM resistivity) is determined principally by the resistivity of the pore fluids (groundwater) in aquifers saturated with high salinity water.

The second step in the calibration process is to mathematically relate chloride to water resistivity. As chloride concentration increases, water resistivity decreases. In groundwater influenced by seawater, the dominant and most conductive ions are chloride and sodium, so it is expected that there will be a statistically strong relationship between water resistivity and chlorides. Again, a log-log plot is constructed with water resistivity of well samples on the x-axis, and chloride ion content of well samples on the y-axis. A regression equation is fitted to the data and has the form:

$$Chlorinity = 2282 \cdot (Water\ Resistivity)^{-1.3019} \qquad (2)$$

with $R^2 = 0.99$, $p < 0.001$, $r > 0.99$. Equations (1) and (2) are combined to form an equation that defines chlorinity as a function of CSEM resistivity. This equation is then used to convert CSEM 3D inversion resistivity to chlorinity.

The log-log plot of CSEM derived chlorinity (x-axis) and lab-determined chloride ion content (y-axis), produces a regression equation with values of $R^2 = 0.91$, $r = 0.96$, and $p < 0.001$. As described above, the p value measures the probability that the observed relationship is due to random variation, R^2 is the percent of the variance in the dependent variable explained by the variance of the independent variable, and *r* measures the strength of the correlation between CSEM determined chlorinity and lab-determined chloride ion content, with an *r* of 1.0 being a perfect correlation (1:1).

The correspondence of chlorinity calculated from CSEM resistivity and lab-derived values of chloride ion content from TPGW wells can be compared to the TPGW well derived chloride values on CSEM-derived chlorinity versus depth profiles. The correspondence of CSEM chlorinity and lab-derived chloride ion content is excellent.

TPGW monitor well data are from the Biscayne Aquifer only; consequently, the calibrated equation relating CSEM resistivity to groundwater chlorinity is valid only for the Biscayne Aquifer. For this reason, mapping of the CSEM derived groundwater chlorinity was restricted to the Biscayne Aquifer, as defined by Fish and Stewart (1991). CSEM resistivity obtained for hydrostratigraphic units below the base of the Biscayne cannot be reliably converted to chlorinity values without depth specific water quality data from those units.

2.3 Method Minimum Reliable Chloride Concentration

The CSEM time-domain resistivity survey at PTN was designed to map the extent of pore waters with greater than 19,000 mg/L chloride ion content as the predominant bulk resistivity response at those concentrations is directly attributable to chloride within the formation of the Biscayne Aquifer. Using the CSEM acquisition and analysis methods employed at PTN to map pore water chloride ion content less than 19,000 mg/L requires an evaluation of the reliable lower method limit. As the chloride ion content of pore waters in the Biscayne Aquifer decreases, the influence of porosity variations on the bulk conductivity of the bedrock/porewater combination increases. At some lower limit of chloride ion content, the geologic noise from porosity variations becomes too large for reliable mapping of chloride ion content using the CSEM method.

To determine the lower limit for reliable mapping of chloride ion values using the CSEM method the accuracy of predicting pore water chloride ion values for waters with chloride levels less than 19,000 mg/L was compared to the accuracy of mapping chloride for waters >19,000 mg/L. Prediction accuracy is defined as the ratio of CSEM predicted chloride to the chloride level of water quality samples obtained at monitor wells. The average CSEM prediction accuracy for subsets of the entire survey dataset were compared to the average prediction accuracy for the entire dataset. The subsets were for water quality samples <19,000 mg/L, <10,000 mg/L, and <5,000 mg/L, and the associated CSEM chloride predictions. The change in predictive error as higher chloride values are added

to the data subset is used as the criterion for selecting a lower limit for reliable prediction of chloride ion content of pore waters.

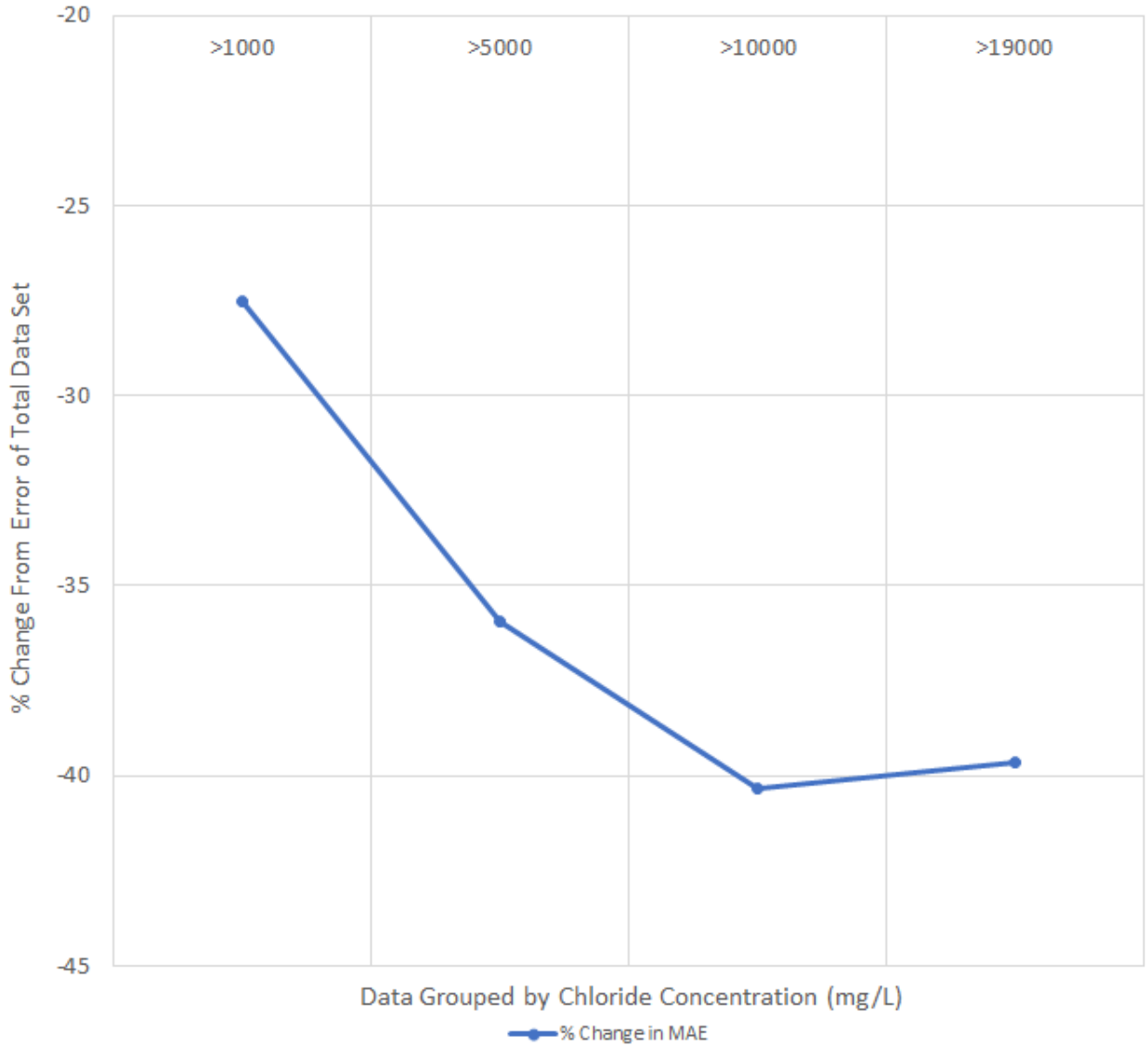

Figure 2.2: Percent Change in Error for Various Chloride Concentration Data Sets

Using this analysis method, the change in average prediction error is the same for data subsets >10,000 mg/L and >19,000 mg/L (Figure 2.2), compared to the average prediction error for the entire dataset. The conclusion is that the average CSEM chloride ion prediction error is about the same for pore waters with chloride ion contents >10,000 mg/L as for pore waters with chloride ion contents >19,000 mg/L. Prediction accuracy decreases significantly for pore water chloride ion contents <10,000 mg/L. Based on this analysis, the reliable lower limit of the CSEM TEM survey for mapping chloride ion content within the Biscayne Aquifer is 10,000 mg/L.

2.4 Presentation of Findings

The information is processed to produce CSEM chloride concentration estimates of the hypersaline groundwater along a specific transect at a specified depth layer in plan view (Figures 3-1 through 3-3), three-dimensional view (Figure 3-4), and cross-sectional view (Figures 3-5 through 3-6). Comparisons of CSEM derived chloride concentrations to measured monitoring well chloride concentrations are shown on Figures 3-7 through 3-14. The data is processed into a three-dimensional grid with defined grid cells, or "Voxels". The CSEM derived chloride concentration values were interpolated to a uniform voxel grid to allow for more effective graphical visualization of the chloride ion distribution and to estimate the volume of material containing hypersaline groundwaater. Each voxel has lateral (x, y) dimensions of 328 x 328 feet (100 x 100 m) and a thickness equivalent to the corresponding layer in the 3D CSEM resistivity layers. The voxel grid is restricted to the thickness of the Biscayne Aquifer, derived from Fish and Stewart (1991) and utilizes layers 1 through 14 of the CSEM 3D model. The 3D CSEM model has 14 layers in the Biscayne Aquifer, ranging in thickness from 1 m (3.3 ft) in Layer 1 to 3.9 m (12.8 ft) in Layer 14. The bottom of layer 14 is at a depth of about 100 feet below land surface (30.3 m).

The range of chloride concentration is displayed as a color spectrum ranging from blue (approximately 18,000 mg/L) to red (approximately 40,000 mg/L). The data can be organized and displayed in a number of ways. Data collected at different layers below ground surface (bgs) along a specific transect can be combined to create two-dimensional "slices" illustrating the vertical variation of salinity within the aquifer. Similarly, data collected within a single layer can be combined to create a two-dimensional plan view of the horizontal salinity variation within the aquifer at the specified depth. Finally, the data can be combined to create three-dimensional representations.

3.0 Findings

3.1 Extent and Estimated Volume of Hypersaline Ground Water

The maximum extent of hypersaline groundwater westward from the CCS is illustrated in Figure 3-2 associated with layer 10, approximately 44 to 55 feet bgs. The maximum westward extent of the hypersaline groundwater is approximately 16,000 feet (4,900 m) west from the west margin of the CCS at a depth of 44 to 55 feet. The hypersaline plume is wedge shaped, with the tip of the wedge at about 55 feet below land surface. At both shallower and deeper depths, the plume does not extend as far west. Along the upper monitoring horizon, represented by survey layer 7 (Figure 3-1), the plume extends about 6,200 feet westward (1,900 m) from the southern portion of the CCS. At the base of the Biscayne Aquifer, represented by layer 14 (Figure 3-3), the plume extends about 5,600 feet westward (1,700 m) from the CCS. Similar to the results in the 2016 CSEM survey, the 2018 baseline survey identified shallow areas of hypersaline groundwater in the upper 5 meters of the aquifer near the coastline. This is an area where bay tidal waters are concentrated by evaporation during the dry season producing hypersaline water which seeps into the groundwater.

3.2 Estimated Volume of CCS Hypersaline Ground Water

The baseline volume of the material with chloride concentrations greater than 19,000 mg/L within the compliance area west and north of the FPL property as identified in the MDC CA is estimated to be 450,493,000 m^3. The estimate sums the volume of each model cell within the 3D voxel model having an estimated chloride concentration of 19,000 mg/L and greater. Figure 3.4 provides a three-dimensional representation of the hypersaline plume west and north of the FPL property.

4.0 References

ENERCON 2016. PTN Cooling Canal System, Electromagnetic Conductance Geophysical Survey, DRAFT FINAL REPORT, Florida Power and Light Turkey Point Power Plant, 9700 SW 433th Street, Homestead, FL 33035

Fish, J. E., and M. Stewart, 1991. Hydrogeology, aquifer characteristics, and ground-water flow of the surficial aquifer system, Dade County, Florida. U.S. Geological Survey, Water Resources Inv. 91-4000.

Fitterman, David V.; Prinos, Scott T., 2011. Results of time-domain electromagnetic soundings in Miami-Dade and southern Broward Counties, Florida. U.S. Geological Society Open-File Report 2011-1299, ix, 42 p.

Fitterman, David V.; Deszcz-Pan, Maria; Prinos, Scott T., 2012. Helicopter Electromagnetic Survey of the Model Land Area, Southeastern Miami-Dade County, Florida. U.S. Geological Society Open-File Report 2012–1176, 77 p.

Prinos, Scott T.; Wacker, Michael A.; Cunningham, Kevin J.; Fitterman, David V., 2014. Origins and delineation of saltwater intrusion in the Biscayne aquifer and changes in the distribution of saltwater in Miami-Dade County, Florida. U.S. Geological Survey Scientific Investigations Report 2014-5025, Report: xi, 101 p.

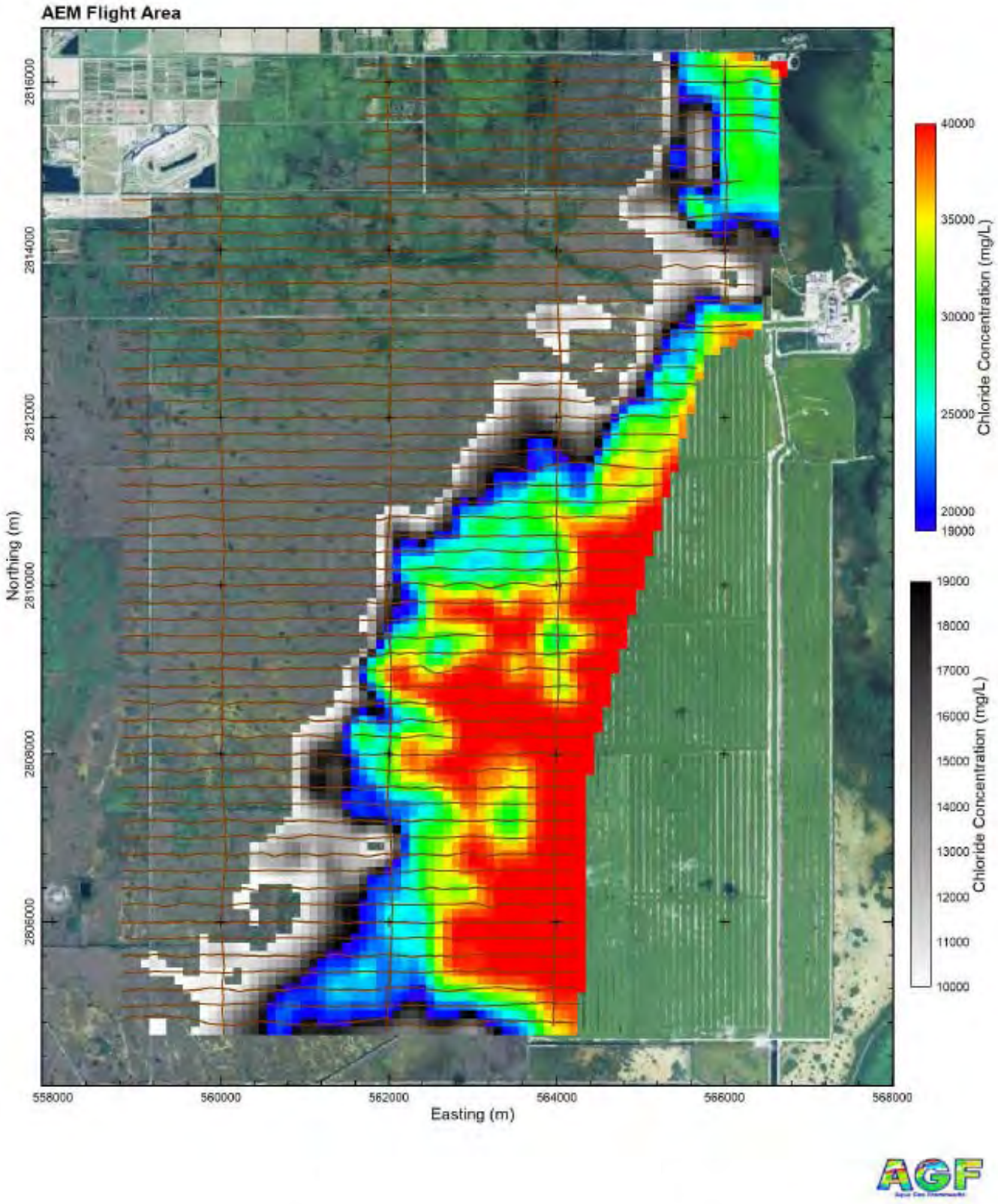

Figure 3-1. Plan View of hypersaline groundwater within Layer 7, between 26 and 32 feet below ground surface (bgs)

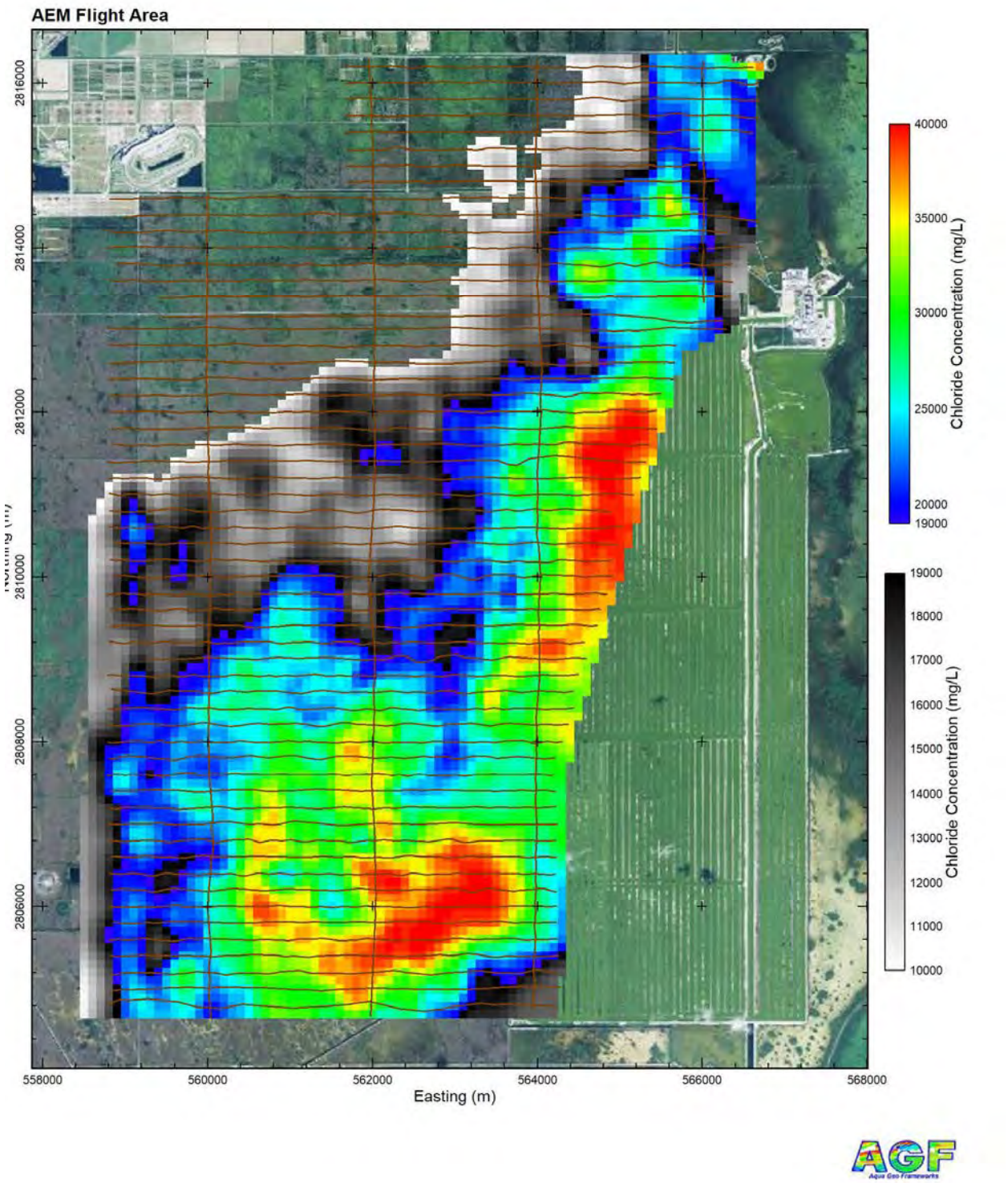

Figure 3-2. Plan View of hypersaline groundwater within Layer 10, between 44 and 55 feet below ground surface (bgs)

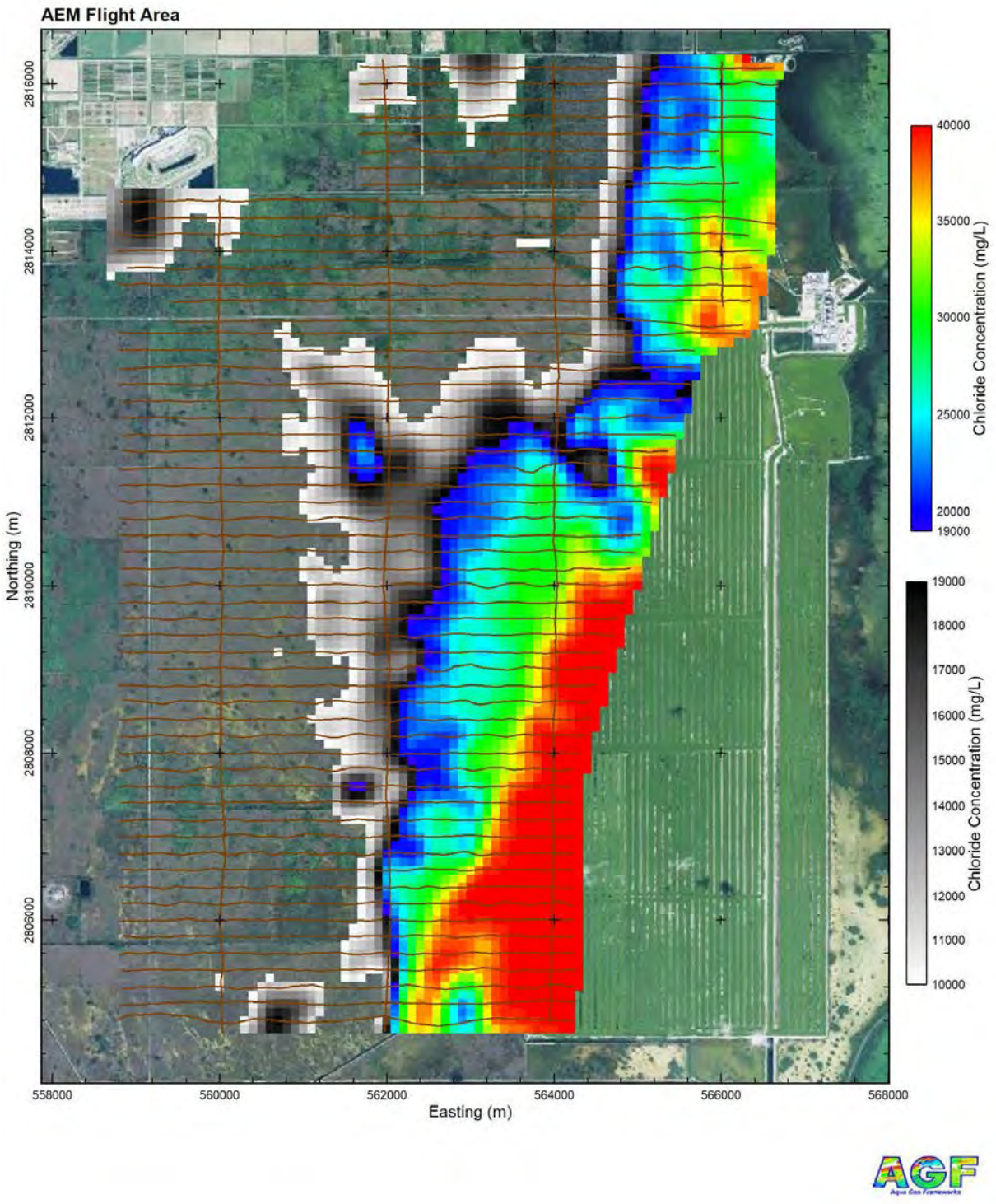

Figure 3-3. Plan View of hypersaline groundwater within Layer 14, between 87 and 99 feet below ground surface (bgs)

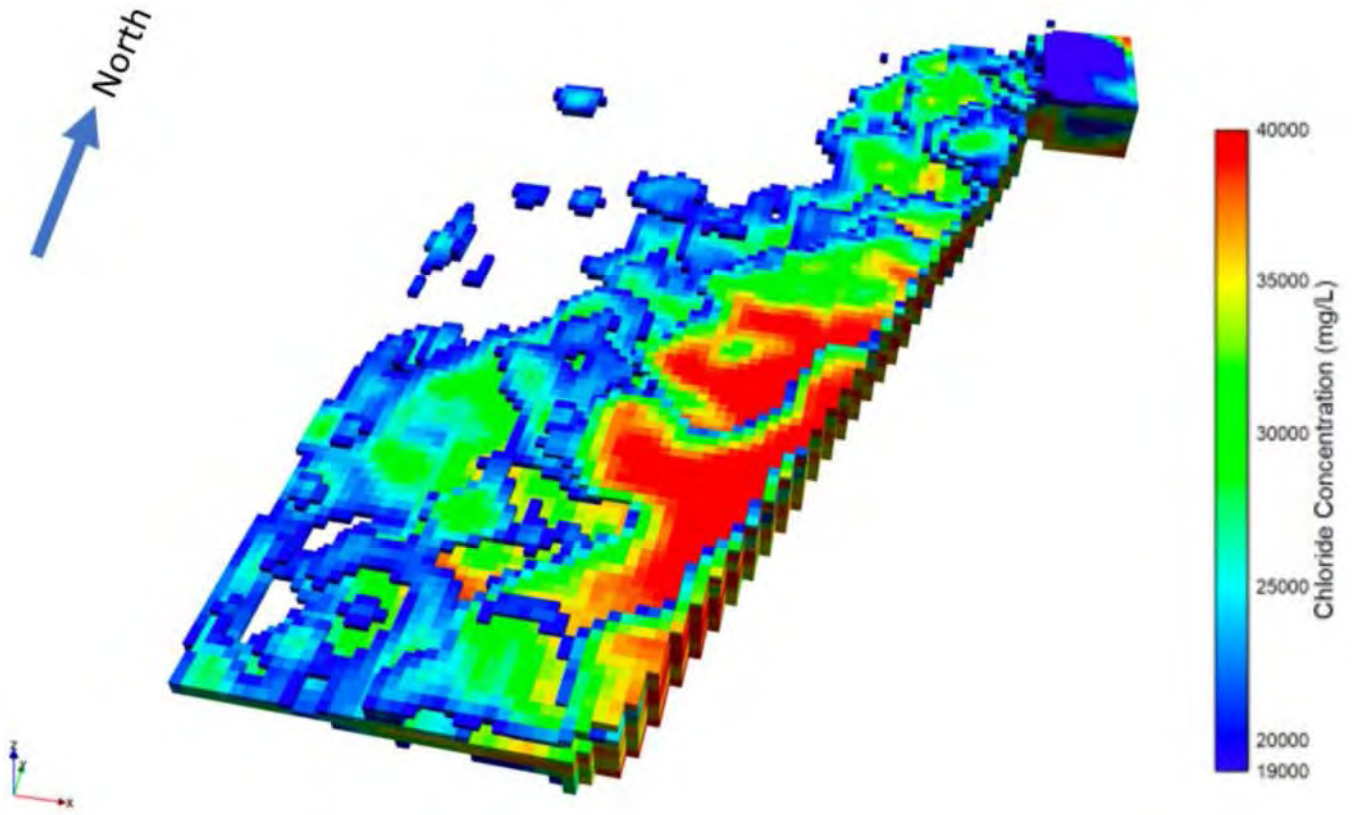

Figure 3-4. Three-Dimensional representation of hypersaline groundwater between 0 and 99 feet below ground surface (bgs)

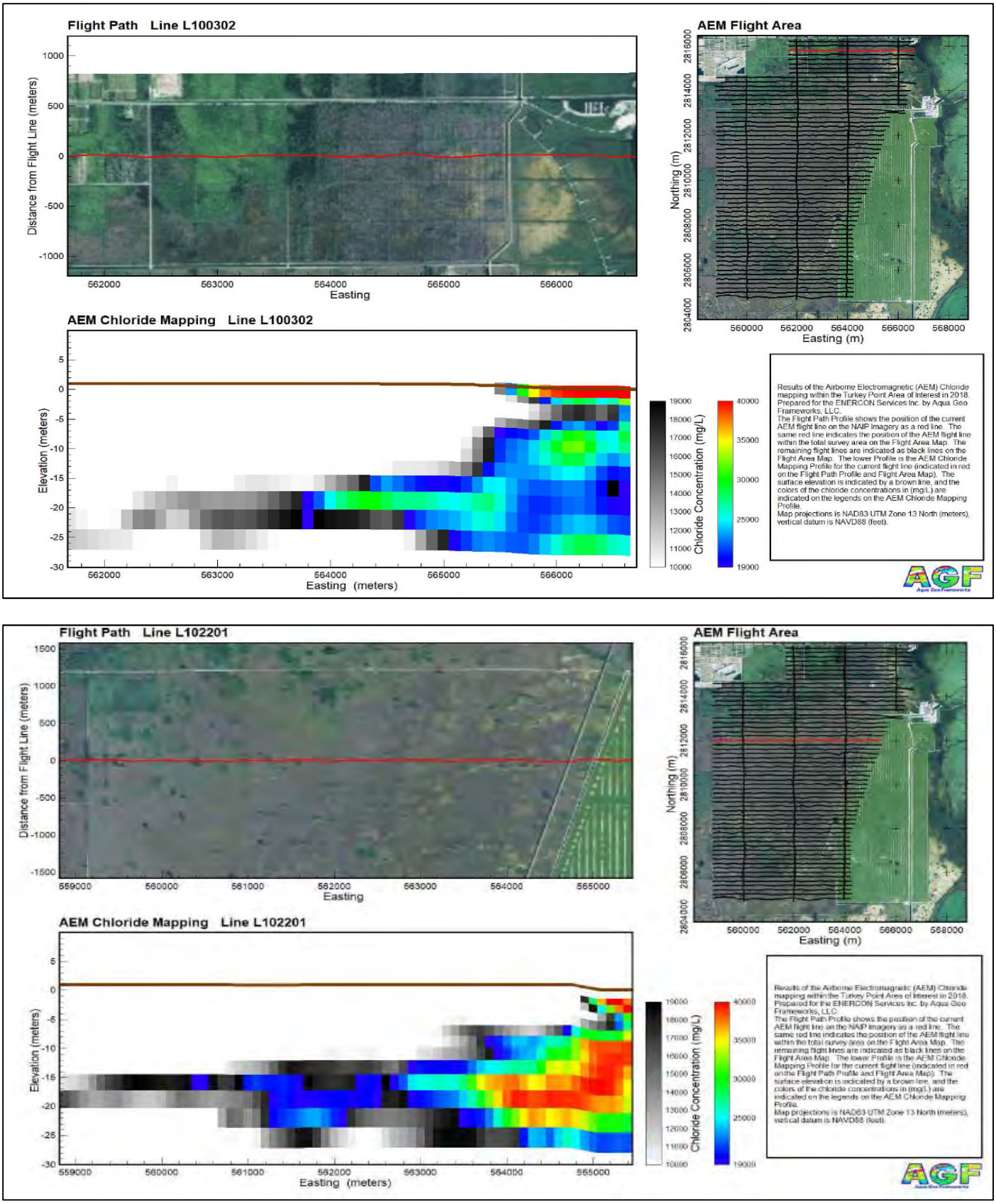

Figure 3-5. Cross sectional chloride profiles: flight lines 100302 and 102201

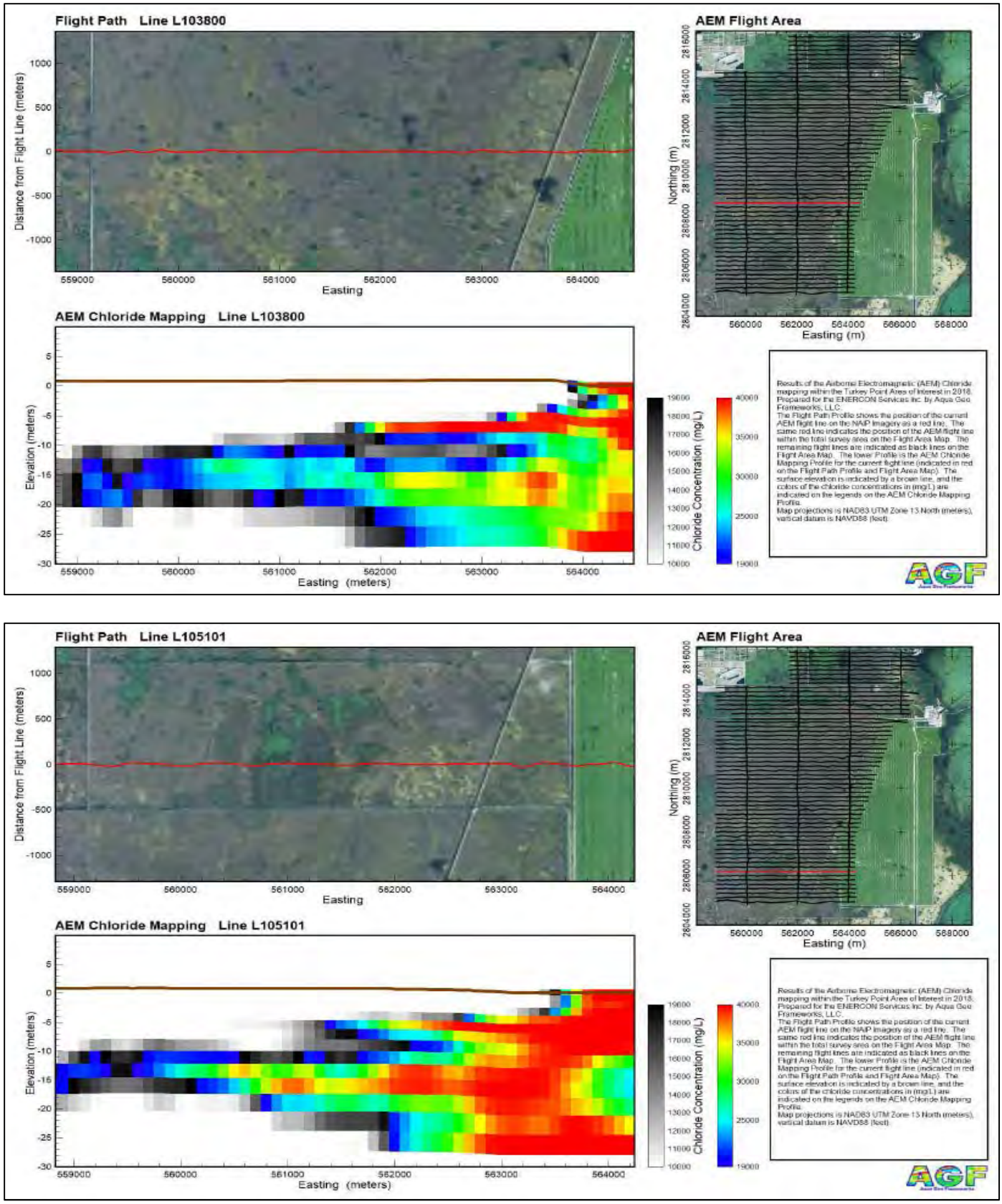

Figure 3-6. Cross sectional chloride profiles: flight lines 103800 and 105101

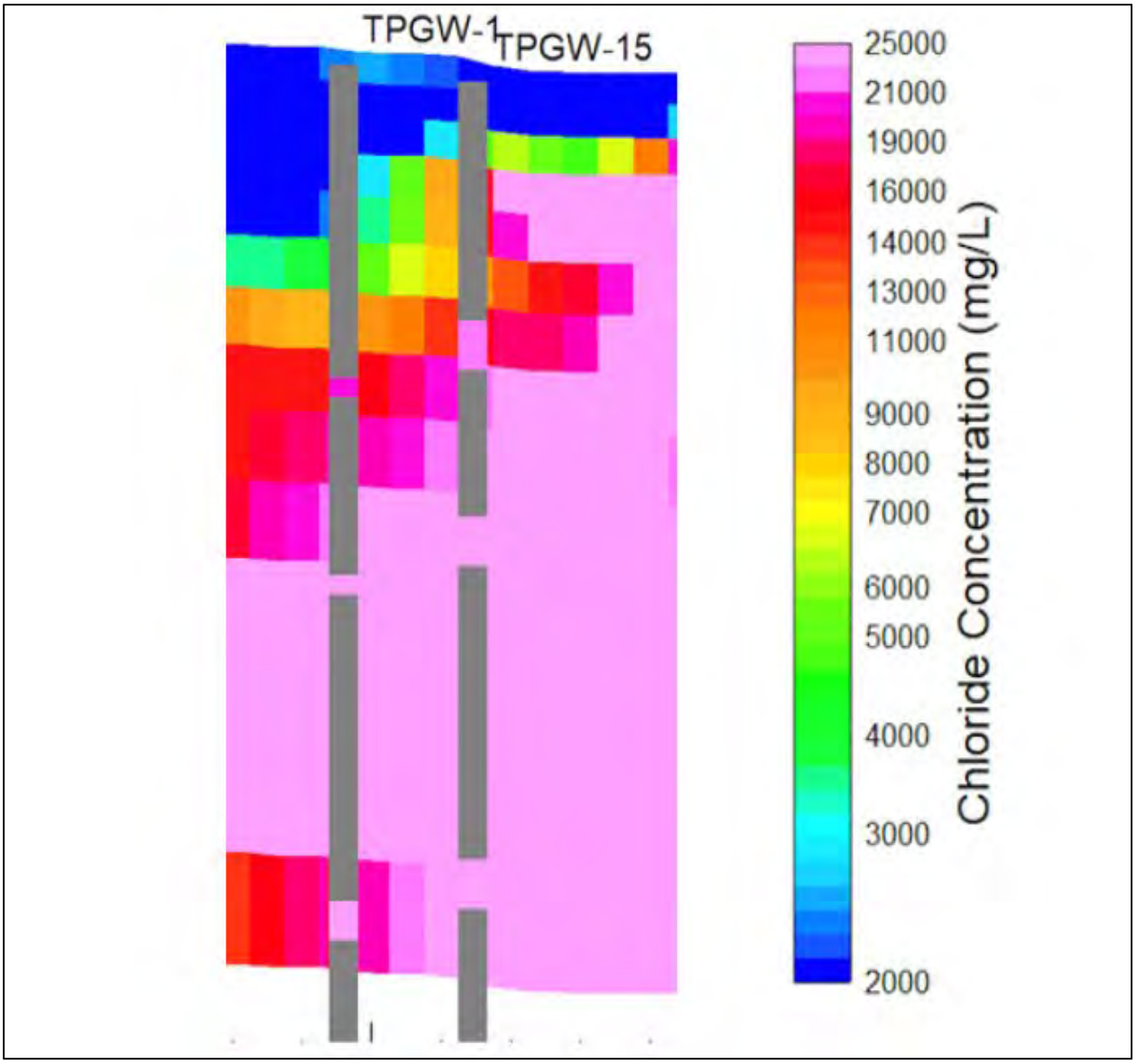

Figure 3-7. Comparison of TEM estimated chloride concentrations with TPGW -1 and TPGW-15. Grey color represents well casings. Measured chloride concentration in the monitoring wells is color coded consistent with the scale on the right

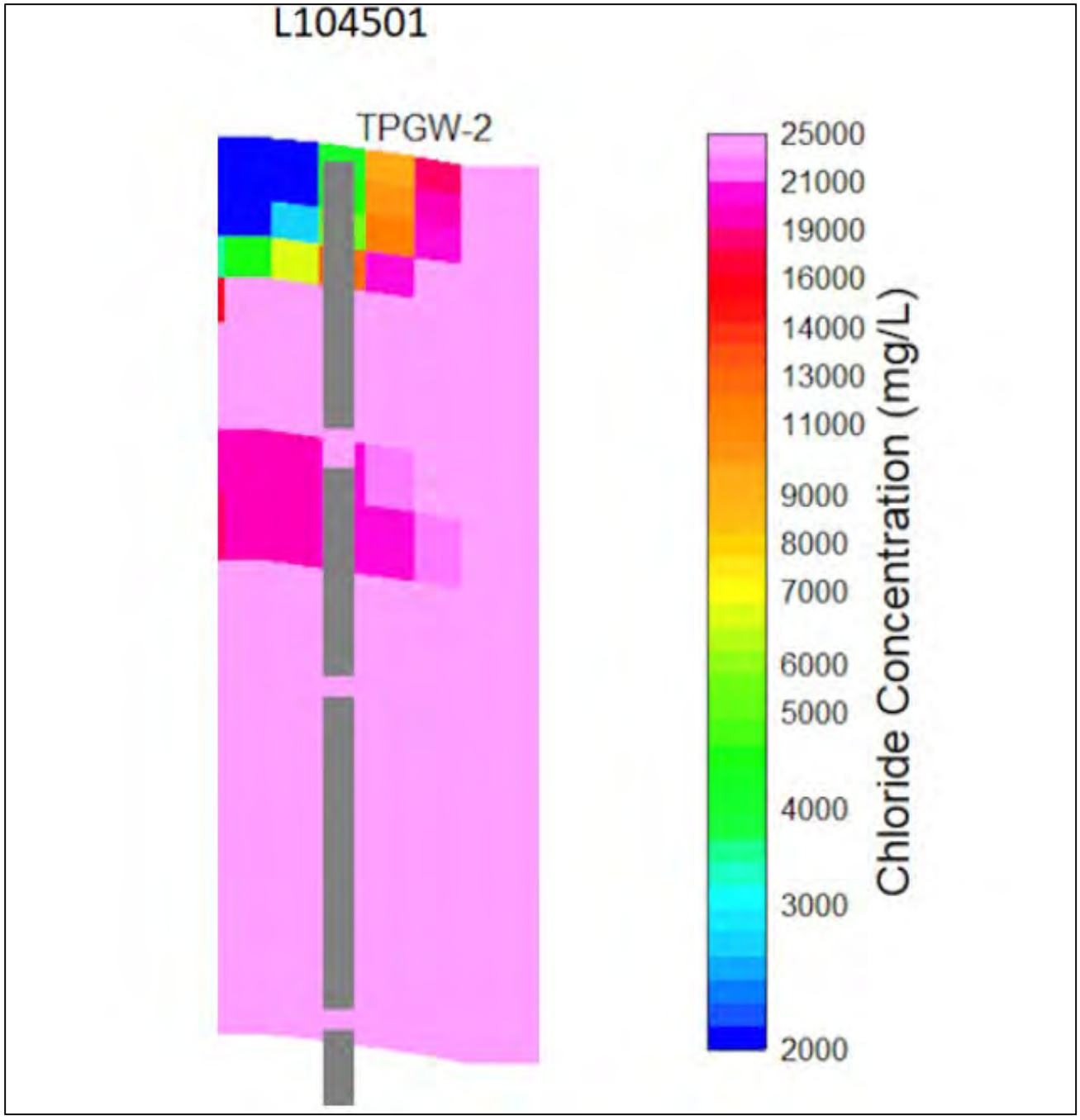

Figure 3-8. Comparison of TEM estimated chloride concentrations with TPGW -2. Grey color represents well casings. Measured chloride concentration in the monitoring wells is color coded consistent with the scale on the right

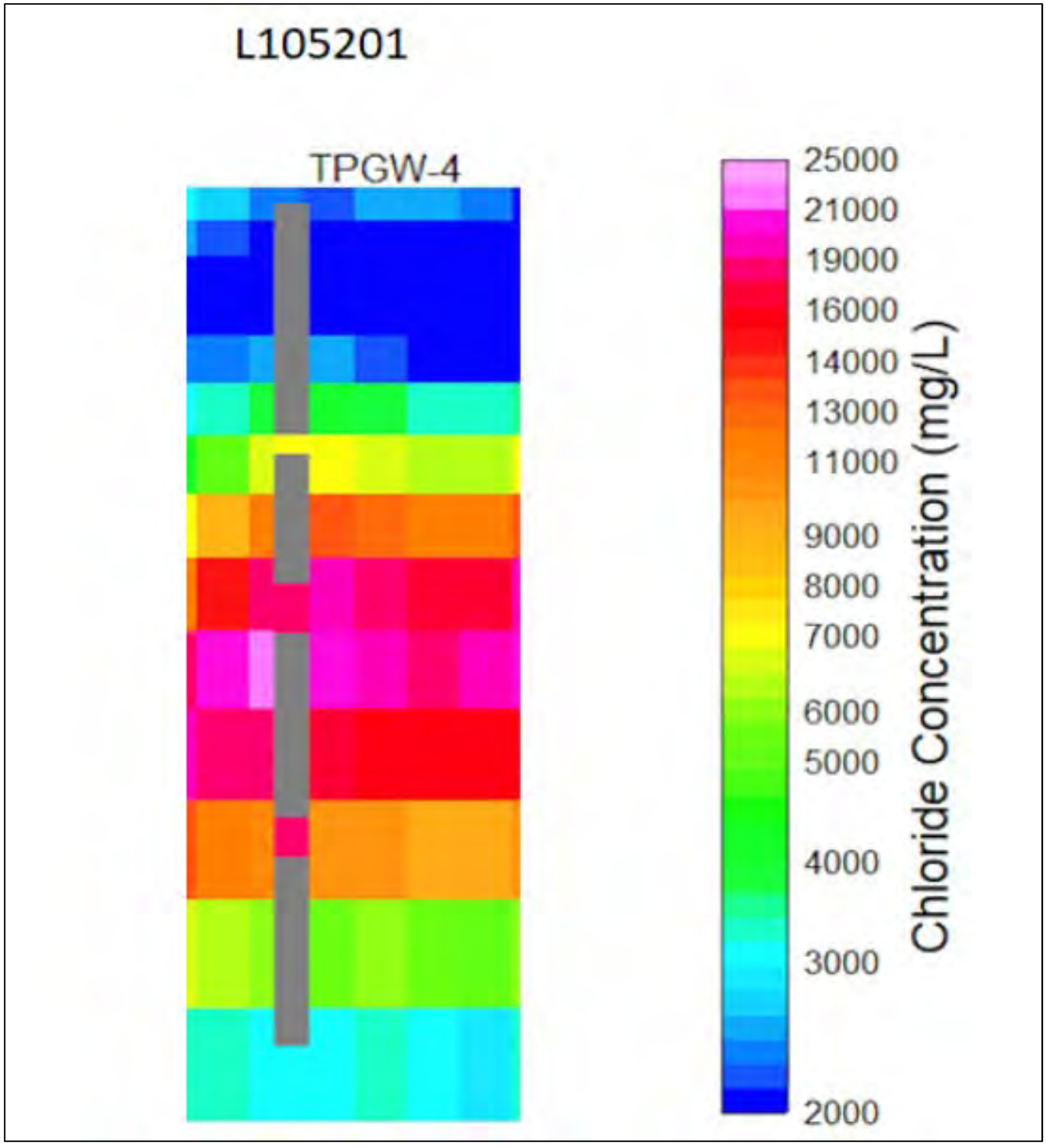

Figure 3-9. Comparison of TEM estimated chloride concentrations with TPGW -4. Grey color represents well casings. Measured chloride concentration in the monitoring wells is color coded consistent with the scale on the right

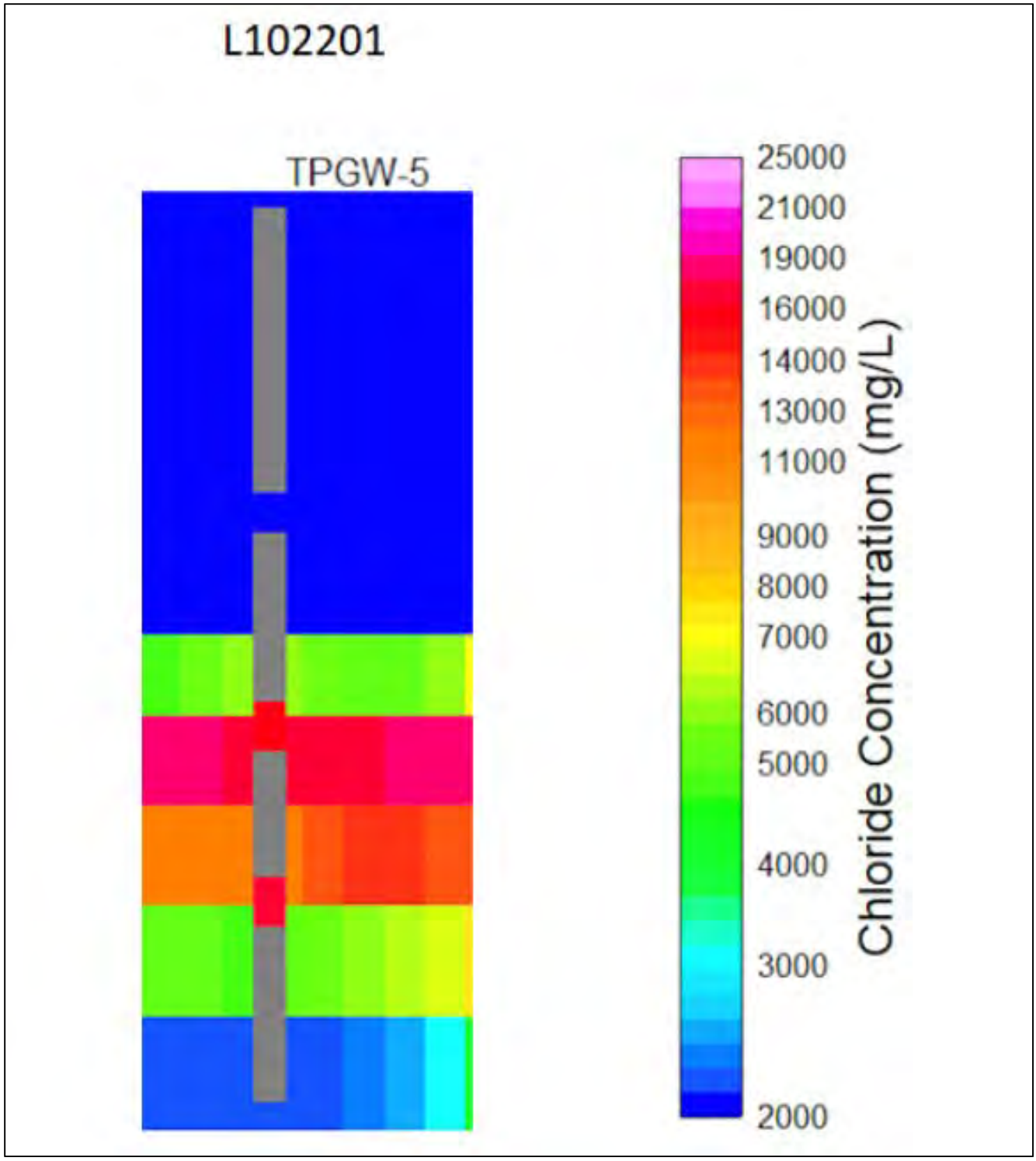

Figure 3-10. Comparison of TEM estimated chloride concentrations with TPGW -5. Grey color represents well casings. Measured chloride concentration in the monitoring wells is color coded consistent with the scale on the right